Available online at www.sciencedirect.com
SCIENCE DIRECT®
Advances in Water Resources 27 (2004) 31–45
Advances in Water Resources
www.elsevier.com/locate/advwatres

MODFLOW equipped with a new method for the accurate simulation of axisymmetric flow

N. Samani [a,*], M. Kompani-Zare [a], D.A. Barry [b]

[a] Department of Earth Sciences, College of Sciences, Shiraz University, Shiraz 71454, Iran
[b] Contaminated Land Assessment and Remediation Research Centre, Institute for Infrastructure and Environment, School of Engineering and Electronics, The University of Edinburgh, Edinburgh EH9 3JN, UK

Received 12 May 2003; received in revised form 21 September 2003; accepted 25 September 2003

Abstract

Axisymmetric flow to a well is an important topic of groundwater hydraulics, the simulation of which depends on accurate computation of head gradients. Groundwater numerical models with conventional rectilinear grid geometry such as MODFLOW (in contrast to analytical models) generally have not been used to simulate aquifer test results at a pumping well because they are not designed or expected to closely simulate the head gradient near the well. A scaling method is proposed based on mapping the governing flow equation from cylindrical to Cartesian coordinates, and vice versa. A set of relationships and scales is derived to implement the conversion. The proposed scaling method is then embedded in MODFLOW 2000. To verify the accuracy of the method steady and unsteady flows in confined and unconfined aquifers with fully or partially penetrating pumping wells are simulated and compared with the corresponding analytical solutions. In all cases a high degree of accuracy is achieved.

Keywords: Groundwater modelling; Radial flow simulation; Groundwater hydraulics; Flow to a well

1. Introduction

The simulation of radial or cylindrical flow to a pumping well has been used by many investigators to determine aquifer properties and determine heads and flows in the vicinity of the well [1,3,6,8,10–13,15]. Simulation of the flow near the well requires that the changes in the head gradient due to radial convergence of flow lines are accurately represented. Widely used finite-difference models such as MODFLOW [5] that are constructed using a rectilinear grid geometry generally have not been used to simulate aquifer test results from a pumping well because they are not designed or expected to closely simulate head changes in pumping wells. Head gradients in the vicinity of the pumping well are large and commonly are underestimated in conventional discretization schemes because distances between adjacent cell centres, or cells next to the well, are too large to capture steep and rapidly changing head gradients. Also the radial geometry of flow, wells and axisymmetric flow boundaries is difficult to simulate by rectilinear grid geometry.

An axisymmetric node-centred scheme for MODFLOW (RADMOD) was presented by Reilly and Harbaugh [13]. Although it is very efficient, it adopts a mesh spacing with a constant expansion factor in the radial direction. The mesh may not coincide with some nodes of interest, a situation that would extend to other MODFLOW packages, such as the Recharge package. Also, RADMOD is not wholly suitable for simulation of unconfined aquifers as it cannot handle drying. These cause considerable errors in the simulation of radial flow in unconfined aquifers when head loss is considerable relative to the aquifer saturated thickness.

Another method for simulating symmetric and non-symmetric flow to pumping wells was presented by Barrash and Dougherty [1]. Their scheme is empirical and based on a trail-and-error procedure with a suggested expansion factor of 1.2–1.5 for the mesh spacing in the Cartesian coordinate system with rectilinear cells. The expansion factor is a constant ratio that can be considered between the dimension of the successive cells in a certain direction in a model [1]. The expansion factor reduces the numerical error due to flow concentration

* Corresponding author. Tel./fax: +98-711-428-4572.
E-mail address: samani@susc.ac.ir (N. Samani).

0309-1708/$ - see front matter © 2003 Elsevier Ltd. All rights reserved.
doi:10.1016/j.advwatres.2003.09.005

Nomenclature

b	aquifer thickness (m)
d	depth from top of the aquifer (m)
x	longitudinal horizontal coordinate in the c-system (m)
y	transverse horizontal coordinate in the c-system (m)
z	vertical coordinate (m)
r	radial coordinate in the r-system (m)
r_D	dimensionless radial coordinate (r/b or r/d)
θ	azimuth angle in the r-system (radian) (Fig. 1)
R	radial coordinate in the R-system, $R = \ln(r)$
H (or ϕ)	hydraulic head (m)
h_0	initial hydraulic head (m)
k_h	horizontal hydraulic conductivity (m/s)
k_v	vertical hydraulic conductivity (m/s)
Q	total discharge of the well (m^3/s)
Q_x	discharge along the x-axis (m^3/s)
Q_y	discharge along the y-axis (m^3/s)
Q_z	discharge along the z-axis (m^3/s)
Q_r	discharge along the r-axis (m^3/s)
$Q_{r\theta}$	discharge along $r\theta$ (horizontal and perpendicular to the r-axis) (m^3/s)
Q_R	discharge along the R-axis (m^3/s)
Q_θ	discharge along θ (horizontal and perpendicular to the R-axis) (m^3/s)
V_x	velocity along the x-axis (m/s)
V_y	velocity along the y-axis (m/s)
V_z	velocity along the z-axis (m/s)
V_r	velocity along the r-axis (m/s)
$V_{r\theta}$	velocity along $r\theta$ (m/s)
V_R	velocity along the R-axis (m/s)
V_θ	velocity along θ in R-system (m/s)
$\Re$	surface recharge to an unconfined aquifer (m/s)
r_w	well radius (m)
n	effective porosity
s	drawdown (m)
S_s	specific storativity (m^{-1})
S_y	specific yield
t	time (s)
T	transmissivity ($k_h b$ or $k_h d$)

and high hydraulic gradient in the vicinity of wells. Here, we propose a method that is theoretically based on geometry and physical properties of aquifer flow. The flow parameters for each cell are established using derived scale factors so that the mesh spacing is not dictated by the user but by the flow conditions.

In the following, we compare the governing equations of groundwater flow in cylindrical and Cartesian coordinates, and so establish relationships between them. By application of these relationships, axisymmetric flow in cylindrical coordinates can be converted to the corresponding flow conditions in Cartesian coordinates. Then, we can apply the conventional rectilinear grid geometry for simulating this converted Cartesian system. By applying these conversions, we obtain an equivalent two-dimensional flow that can be simulated with rectilinear grid geometry. Next, this approach is adopted in MODFLOW such that the radial flow simulations are compatible with all packages within this widely used software. Our approach could also be used with other finite difference numerical models.

2. Flow equations and parameters in cylindrical and Cartesian coordinates

Assume that a solution has been derived for a given flow problem in a two-dimensional Cartesian system. This may be either an analytical solution of the governing flow equations subjected to a given set of initial and boundary conditions or a solution obtained by using a numerical model or other analogue which simulates two-dimensional flow. In the following we derive some relationships by which these solutions may also be applied to radial flow conditions. On the other hand, a solution for a radial flow system may be given. Again, solution may be obtained by transformation into an equivalent two-dimensional flow system, solved there, then transferred back to the given radial flow system.

The derivation of the required relationships is based on mapping the governing equations and boundary conditions for two-dimensional flow in Cartesian and cylindrical coordinates.

Three cases will be considered:

1. Steady flow in a confined aquifer.
2. Unsteady flow in a confined aquifer.
3. Unsteady flow in an unconfined aquifer, with or without accretion.

At steady state, the elasticity of liquid and medium is neglected. In unsteady-confined flow the effect of specific storage and in unsteady-unconfined case the effect of specific yield, and aquifer saturated thickness is taken into account. For this work, the aquifer is homogeneous, horizontal and of infinite extent but the proposed method can also be used for the aquifers with axisymmetric nonhomogenities, like horizontal layered aquifers and also for the case that the flow is bounded by axisymmetric boundaries. It must be noted that in many

cases the aquifer nonhomogenities in the vicinity of the well may be treated as axisymmetric. And also an axisymmetric flow model can better simulate the well boundaries like well skin especially in the case of large diameter wells.

2.1. Changing the cylindrical coordinate flow system to an equivalent Cartesian coordinate flow system

To transform the cylindrical coordinate flow system to an equivalent Cartesian coordinate flow system, we have to determine the relation between all parameters in the two flow systems. The relation between the parameters can be determined by comparing the corresponding governing equations in the systems. The governing equations in a flow system are continuity equations, elementary discharge equations, average velocity equations and equations expressing boundary conditions. For comparing two corresponding equations, at first they must be identical or they must have the same number of statements in each side. By dividing each corresponding statement in two equations the ratio between corresponding statements will be obtained. The number of obtained ratios is the same as the number of statements in each equation. Equalising the ratio between the statements, the relation between parameters in the two systems will be derived.

In the following discussion, subscript r denotes values in the cylindrical coordinate system, subscript R denotes values in the radial flow system whose r coordinate is replaced by $R = \ln(r)$, subscript c denotes values in the two-dimensional (Cartesian coordinate) equivalent flow system and subscript p denotes the ratio of the values in the two-dimensional flow c-system to the corresponding value in the radial flow R-system. If the Cartesian coordinate system x, y and z (with z vertically upward) and the cylindrical coordinate systems r, θ and z and R, θ and z with $R = \ln(r)$, are employed, then relevant ratios between the parameters in R and c-systems are (see Fig. 1):

$$x_p = \frac{\partial x_c}{\partial R}; \quad y_p = \frac{\partial y_c}{\partial \theta}; \quad z_p = \frac{\partial z_c}{\partial z_R}; \quad k_{hp} = \frac{k_{hc}}{k_{hR}};$$
$$k_{vp} = \frac{k_{vc}}{k_{vR}}; \quad \phi_p = \frac{\partial \phi_c}{\partial \phi_R}; \quad Q_{rp} = \frac{\partial Q_{xc}}{\partial Q_{rR}}, \quad \text{etc.}$$

2.1.1. Summary of basic equations

2.1.1.1. Continuity equations. Because, the time parameter does not exist in the governing equations for steady flow, we treat the steady and unsteady flow equations separately.

For steady state flow in confined aquifer the continuity equations in cylindrical coordinate system (r-system) and Cartesian coordinate system (c-system) are as follows [2]:

$$k_{hr}\frac{1}{r^2}\frac{\partial^2 \phi_r}{\partial \theta^2} + k_{vr}\frac{\partial^2 \phi_r}{\partial z_r^2} + k_{hr}\frac{\partial^2 \phi_r}{\partial r^2} + k_{hr}\frac{1}{r}\frac{\partial \phi_r}{\partial r} = 0, \tag{1a}$$

$$k_{hc}\frac{\partial^2 \phi_c}{\partial y_c^2} + k_{hc}\frac{\partial^2 \phi_c}{\partial x_c^2} + k_{vc}\frac{\partial^2 \phi_c}{\partial z_c^2} = 0. \tag{1b}$$

As can be seen Eqs. (1a) and (1b) do not have the same number of statement in the left side. To make the two equations identical we introduce R-system and rewrite Eq. (1a) in term of R ($R = \ln(r)$) instead of r, as follows:

$$k_{hR}e^{-2R}\frac{\partial^2 \phi_R}{\partial \theta^2} + k_{hR}\frac{\partial^2 \phi_R}{\partial R^2}e^{-2R} + k_{vR}\frac{\partial^2 \phi_R}{\partial z_R^2} = 0 \tag{1c}$$

Now Eqs. (1c) and (1b) have the same number of statements and are identical.

The above continuity equations, for unsteady flow in a confined aquifer for the three r, R and c-systems become:

$$k_{hr}\frac{1}{r^2}\frac{\partial^2 \phi_r}{\partial \theta^2} + k_{vr}\frac{\partial^2 \phi_r}{\partial z_r^2} + k_{hr}\frac{\partial^2 \phi_r}{\partial r^2} + k_{hr}\frac{1}{r}\frac{\partial \phi_r}{\partial r} = S_{sr}\frac{\partial \phi_r}{\partial t_r}, \tag{2a}$$

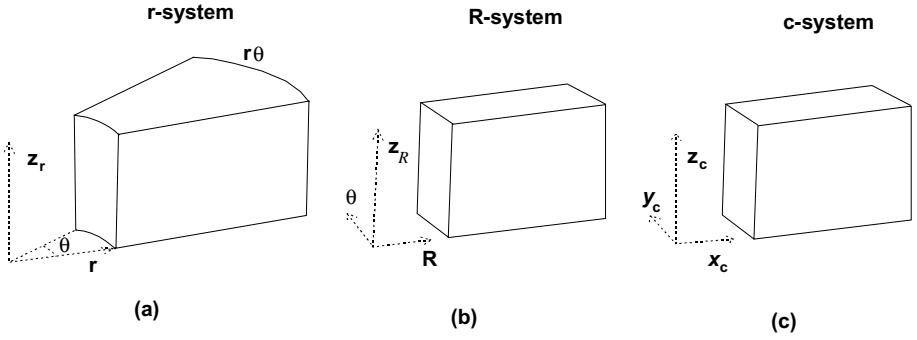

Fig. 1. (a) Cylindrical coordinate system (r-system) which is converted to (b) two-dimensional R-system. The R-system is identical to the (c) two-dimensional Cartesian coordinate (c-system). r, θ z_r in the r-system are converted to R, θ, z_r in the R-system respectively, which are identical to x_c, y_c, z_c in the c-system.

$$k_{hR}e^{-2R}\frac{\partial^2\phi_R}{\partial\theta^2}+k_{hR}\frac{\partial^2\phi_R}{\partial R^2}e^{-2R}+k_{vR}\frac{\partial^2\phi_R}{\partial z_R^2}=S_{sR}\frac{\partial\phi_R}{\partial t_R} \quad (2b)$$

and

$$k_{hc}\frac{\partial^2\phi_c}{\partial y_c^2}+k_{hc}\frac{\partial^2\phi_c}{\partial x_c^2}+k_{vc}\frac{\partial^2\phi_c}{\partial z_c^2}=S_{sc}\frac{\partial\phi_c}{\partial t_c}. \quad (2c)$$

For the unsteady-unconfined flow similar equation can be written.

2.1.1.2. Elementary discharge equations. Following the above transformation from r to R system, elementary discharge by Darcy's law for the three systems and in all directions is as follows (see Fig. 2):

$$dQ_{rr}=k_{hr}\frac{\partial\phi_r}{\partial r}dz_r\,d\theta_r, \quad (3a)$$

$$dQ_{RR}=k_{hR}\frac{\partial\phi_R}{\partial R}dz_R\,d\theta, \quad (3b)$$

$$dQ_{xc}=k_{hc}\frac{\partial\phi_c}{\partial x_c}dz_c\,dy_c, \quad (3c)$$

$$dQ_{zr}=k_{vr}\frac{\partial\phi_r}{\partial z_r}r\,d\theta\,dr, \quad (3d)$$

$$dQ_{zR}=k_{vR}\frac{\partial\phi_R}{\partial z_R}d\theta\,dR\,e^{2R}, \quad (3e)$$

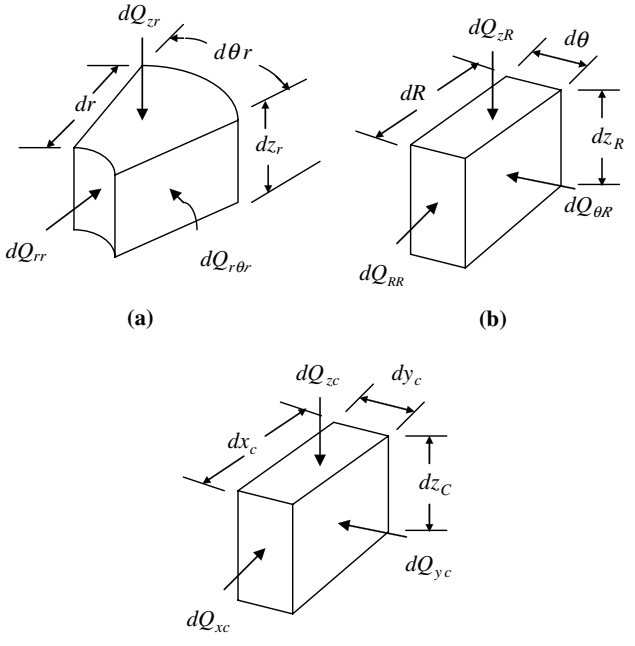

Fig. 2. Schematic diagram showing the relation between the discharge in three directions and the dimensions in (a) r-system, (b) R-system and (c) c-system.

$$dQ_{zc}=k_{vc}\frac{\partial\phi_c}{\partial z_c}dx_c\,dy_c, \quad (3f)$$

$$dQ_{r\theta r}=k_{hr}\frac{\partial\phi_r}{r\partial\theta}dz_r\,dr, \quad (3g)$$

$$dQ_{\theta R}=k_{hR}\frac{\partial\phi_R}{\partial\theta}dR\,dz_R \quad (3h)$$

and

$$dQ_{yc}=k_{hc}\frac{\partial\phi_c}{\partial y_c}dx_c\,dz_c. \quad (3i)$$

2.1.1.3. Average velocity equations. To determine the relation between the time parameter in steady state flow and also the porosity parameter in the two systems, we have to consider the velocity equation in three coordinate directions. The average velocity equations in the three systems and in every coordinate direction are as follows (note that the transformation of equations from r to R system follows the same procedure as above):

$$v_{rr}=\frac{dr}{dt_r}=\frac{k_{hr}}{n_r}\frac{\partial\phi_r}{\partial r}, \quad (4a)$$

$$v_{RR}=\frac{dR}{dt_R}=\frac{k_{hR}}{n_R}\frac{\partial\phi_R}{\partial R}e^{-2R}, \quad (4b)$$

$$v_{xc}=\frac{dx_c}{dt_c}=\frac{k_{hc}}{n_c}\frac{\partial\phi_c}{\partial x_c}, \quad (4c)$$

$$v_{zr}=\frac{dz_r}{dt_r}=\frac{k_{vr}}{n_r}\frac{\partial\phi_r}{\partial z_r}, \quad (4d)$$

$$v_{zR}=\frac{dz_R}{dt_R}=\frac{k_{vR}}{n_R}\frac{\partial\phi_R}{\partial z_R}, \quad (4e)$$

$$v_{zc}=\frac{dz_c}{dt_c}=\frac{k_{vc}}{n_c}\frac{\partial\phi_c}{\partial z_c}, \quad (4f)$$

$$v_{rr}=\frac{r\,d\theta}{dt_r}=\frac{k_{hr}}{n_r}\frac{\partial\phi_r}{r\partial\theta}, \quad (4g)$$

$$v_{\theta R}=\frac{d\theta}{dt_R}=\frac{k_{hR}}{n_R}\frac{\partial\phi_R}{\partial\theta}e^{-2R} \quad (4h)$$

and

$$v_{yc}=\frac{dy_c}{dt_c}=\frac{k_{hc}}{n_c}\frac{\partial\phi_c}{\partial y_c}. \quad (4i)$$

Eqs. (3) and (4) apply for both unconfined and confined aquifers.

2.1.1.4. Boundary conditions. On the phreatic surface the water pressure is zero:

$$\phi_R=z_R \quad \text{and} \quad \phi_c=z_c. \quad (5)$$

The boundary conditions along a phreatic surface with accretion at a constant rate $\Re$ in the z direction are:

$$k_{hr}\left[\frac{\partial^2\phi_r^2}{\partial r^2}+\frac{1}{r}\frac{\partial\phi_r^2}{\partial r}+\frac{1}{r^2}\frac{\partial^2\phi_r^2}{\partial\theta^2}\right]+k_{vr}\left[\frac{\partial^2\phi_r^2}{\partial z_r^2}-\frac{\partial\phi_r}{\partial z_r}\right]+\Re_r\left[\frac{\partial\phi_r}{\partial z_r}-1\right]=n_r\frac{\partial\phi_r}{\partial t_r}, \tag{6a}$$

$$k_{hR}\left[\frac{\partial^2\phi_R^2}{\partial R^2}e^{-2R}+\frac{\partial^2\phi_R^2}{\partial\theta^2}e^{-2R}\right]+k_{vR}\left[\frac{\partial^2\phi_R^2}{\partial z_R^2}-\frac{\partial\phi_R}{\partial z_R}\right]+\Re_R\left[\frac{\partial\phi_R}{\partial z_R}-1\right]=n_R\frac{\partial\phi_R}{\partial t_R} \tag{6b}$$

and

$$k_{hc}\left[\frac{\partial^2\phi_c^2}{\partial x_c^2}+\frac{\partial^2\phi_c^2}{\partial y_c^2}\right]+k_{vc}\left[\frac{\partial^2\phi_c^2}{\partial z_c^2}-\frac{\partial\phi_c}{\partial z_c}\right]+\Re_c\left[\frac{\partial\phi_c}{\partial z_c}-1\right]=n_c\frac{\partial\phi_c}{\partial t_c}, \tag{6c}$$

where n is the effective porosity [2]. It must be noted that if the specific retention of the unconfined aquifer assumed to be equal to zero then the specific yield (S_y) and effective porosity (n) for the system will be the same [2,17]. Other boundary conditions such as specified potential or fluxes along boundaries could also be introduced.

2.2. Relationships between flow parameters in the two systems

The derivation of the required relationships is based on the similarity between the equations governing the flow in the two R and c-systems. Let us introduce the following ratios in the equations of the two systems:

$$x_p=\frac{\partial x_c}{\partial R};\quad y_p=\frac{\partial y_c}{\partial\theta};\quad z_p=\frac{\partial z_c}{\partial z_R};\quad k_{hp}=\frac{k_{hc}}{k_{hR}};$$
$$k_{vp}=\frac{k_{vc}}{k_{vR}};\quad \phi_p=\frac{\partial\phi_c}{\partial\phi_R};\quad Q_{rp}=\frac{dQ_{xc}}{dQ_{rR}}\quad \text{etc.}$$

According to Eqs. (1)–(6), for some parameters like x_p, y_p, z_p, ϕ_p and z_p the ratio is between the difference of the parameters ($\partial x_c/\partial R$) and for the other parameters like k_{hp} and k_{vp} the ratio is between the value of the parameters. To determine the above mentioned ratios for the steady state case we can use the continuity equation for steady state condition in c and R-systems (Eqs. (1c) and (1b)). By dividing each statement of Eq. (1b) by the corresponding statement in Eq. (1c) and substituting into the above ratios, we obtain:

$$\frac{\phi_p}{y_p^2}k_{hp},\quad \frac{\phi_p}{x_p^2}k_{hp},\quad \frac{\phi_p}{z_p^2}k_{vp}e^{-2R}.$$

Then, the corresponding equations in the two systems will become identical if the following relation exists:

$$\frac{\phi_p}{y_p^2}k_{hp}=\frac{\phi_p}{x_p^2}k_{hp}=\frac{\phi_p}{z_p^2}k_{vp}e^{-2R}. \tag{7}$$

which is actually two conditions or equations. Applying the above procedure on Eq. (2) the following equation (three conditions) will be achieved:

$$\frac{\phi_p}{y_p^2}k_{hp}=\frac{\phi_p}{x_p^2}k_{hp}=\frac{\phi_p}{z_p^2}k_{vp}e^{-2R}=\frac{S_{sp}\phi_p}{t_p}e^{-2R}. \tag{8}$$

Similarly for Eq. (3):

$$Q_{Rp}=k_{hp}\frac{\phi_p}{x_p}z_py_p, \tag{9a}$$

$$Q_{zp}=k_{vp}\frac{\phi_p}{z_p}x_py_pe^{-2R} \tag{9b}$$

and

$$Q_{\theta p}=k_{hp}\frac{\phi_p}{y_p}z_px_p. \tag{9c}$$

For Eq. (4):

$$v_{rp}=\frac{x_p}{t_p}=\frac{k_{hp}}{n_p}\frac{\phi_p}{x_p}e^{2R}, \tag{10a}$$

$$v_{zp}=\frac{z_p}{t_p}=\frac{k_{vp}}{n_p}\frac{\phi_p}{z_p} \tag{10b}$$

and

$$v_{\theta p}=\frac{y_p}{t_p}=\frac{k_{hp}}{n_p}\frac{\phi_p}{y_p}e^{2R}. \tag{10c}$$

For Eq. (5):

$$\phi_p=z_p. \tag{11}$$

Finally, for Eq. (6):

$$k_{hp}\left(\frac{\phi_p}{x_p}\right)^2=k_{hp}\left(\frac{\phi_p}{y_p}\right)^2=k_{vp}\left(\frac{\phi_p}{z_p}\right)^2e^{-2R}=k_{vp}\left(\frac{\phi_p}{z_p}\right)e^{-2R}=\Re_pe^{-2R}=\Re_p\left(\frac{\phi_p}{z_p}\right)e^{-2R}=n_p\frac{\phi_p}{t_p}e^{-2R}. \tag{12}$$

Notice that some of the conditions in Eqs. (7)–(12) are interdependent. By using these interdependent conditions one can extract the independent conditions for each case study. The three special cases mentioned in Section 2 will now be considered.

Case 1. Steady flow in a confined aquifer

The flow in this case is governed by Eqs. (1), (3) and (4). The parameters involved are:

R-system: R, θ, z_R, k_{hR}, k_{vR}, Q_{RR}, Q_{zR}, $Q_{\theta R}$, ϕ_R, t_R, n_R (11 parameters)

c-system: x_c, y_c, z_c, k_{hc}, k_{vc}, Q_{xc}, Q_{zc}, Q_{yc}, ϕ_c, t_c, n_c (11 parameters)

The conditions applicable for parameter determination are Eqs. (7), (9) and (10), (eight conditions all together). These conditions are interdependent and from which the independent conditions may be found. Therefore, by Eq. (10):

$$x_p = \left(\frac{t_p}{n_p}\right)^{1/3} Q_{Rp}^{1/3} e^{2/3R} = k_{hp}^{1/2}\left(\frac{t_p\phi_p}{n_p}\right)^{1/2} e^{R}, \tag{13}$$

by Eq. (7):

$$y_p = \left(\frac{t_p}{n_p}\right)^{1/3} Q_{\theta p}^{1/3} e^{2/3R} = k_{hp}^{1/2}\left(\frac{t_p\phi_p}{n_p}\right)^{1/2} e^{R} \tag{14}$$

and

$$z_p = \left(\frac{t_p}{n_p}\right)^{1/3} Q_{zp}^{1/3} e^{2/3R} = k_{vp}^{1/2}\left(\frac{t_p\phi_p}{n_p}\right)^{1/2}; \tag{15}$$

by Eqs. (9a) and (9b):

$$k_{hc} = Q_{Rp}^{2/3}\frac{k_{hR}}{\phi_p}\left(\frac{n_p}{t_p}\right)^{1/3} e^{-2/3R} \tag{16a}$$

and

$$k_{vc} = Q_{zp}^{2/3}\frac{k_{vR}}{\phi_p}\left(\frac{n_p}{t_p}\right)^{1/3} e^{4/3R}. \tag{16b}$$

This means that out of the 11 parameters of the equivalent system, six may be chosen arbitrarily; the other five will be determined by the above five conditions (Eqs. (13)–(16)).

Among the various possible groups of arbitrarily chosen parameters, some are of special interest especially if the *c*-system involved. As an example, consider the following case. We want that the value of the discharge in all directions, the time and the hydraulic head in the two systems be the same. So, we set the value of these parameter ratios to 1 and determine the other parameter ratios using the governing conditions. In this case the six parameters: ϕ_p, Q_{Rp}, Q_{zp}, $Q_{\theta p}$, t_p, n_p are set equal to 1 while the other five parameter ratios are determined by Eqs. (13)–(16) as follows:

$$x_p = k_{hp}^{1/2}; \quad y_p = k_{hp}^{1/2}; \quad z_p = k_{vp}^{1/2}e^{-R}; \quad k_{hc} = k_{hR};$$
$$k_{vc} = k_{vR}e^{2R}; \quad n_p = e^{2R}; \quad \text{etc.}$$

That is, $x_p = 1$, $y_p = 1$, $z_p = 1$, $k_{hp} = 1$, $k_{vp} = e^{2R}$ and $n_p = e^{2R}$.

Case 2. Unsteady flow in a confined aquifer

Eqs. (2)–(4) govern the flow. The parameters involved are: x_c, y_c, z_c k_{hc}, k_{vc}, t_c, n_c, Q_{cx}, Q_{cy}, Q_{cz}, ϕ_c and S_{sc} (12 parameters). Conditions Eq. (8) (three conditions), Eq. (9) (three conditions) and Eq. (10) (three conditions) hold. These conditions are interdependent and from them the independent conditions can be derived. The independent conditions Eqs. (13)–(16) are obtained for this case plus condition:

$$S_{sp} = \frac{n_p}{\phi_p} \tag{17}$$

which is derived from Eq. (8) and (10). Here we have six independent condition or equation and 12 unknown. Again, this means that six parameters may be chosen arbitrarily. For example, if we choose Q_{Rp}, Q_{zp}, $Q_{\theta p}$, t_p, z_p and σ_p, we shall have n_p, k_{hc}, k_{vc}, S_{sp}, y_p and x_p from the six above conditions (Eqs. 13–17). A suitable and convenient choice is

$$Q_{Rp} = 1; \quad Q_{zp} = 1; \quad Q_{\theta p} = 1; \quad t_p = 1;$$
$$\phi_{p=}1; \quad z_p = 1.$$

Then

$$n_p = \frac{k_{hc}}{k_{hR}}e^{2R}; \quad k_{hc} = k_{hR}; \quad k_{vc} = k_{vR}e^{2R};$$
$$S_{sp} = \frac{k_{hc}}{k_{hR}}e^{2R}; \quad y_p = 1; \quad x_p = 1.$$

That is, $x_p = 1$, $y_p = 1$, $k_{hp} = 1$, $k_{vp} = e^{2R}$, $S_{sp} = e^{2R}$ and $n_p = e^{2R}$.

Case 3. Unsteady flow in an unconfined aquifer, with and without vertical accretion

The governing equations are Eq. (9) (three conditions), Eq. (10) (three conditions), Eqs. (11) and (12) (eight conditions). These conditions are interdependent. The following independent condition can be derived from them:

from Eq. (11),

$$z_p = \phi_p, \tag{18}$$

from Eqs. (9) and (12),

$$x_p = \frac{Q_{Rp}}{k_{hp}\phi_p} \tag{19a}$$

$$y_p = \frac{Q_{\theta p}}{k_{hp}\phi_p}, \tag{19b}$$

from Eq. (9),

$$k_{hc} = \frac{Q_{Rp}k_{hp}}{\phi_p^2} \tag{20a}$$

$$k_{vc} = \frac{Q_{zp}k_{vR}k_{vp}}{\phi_p^2 k_{hp}}, \tag{20b}$$

from Eq. (10),

$$t_p = \frac{n_p\phi_p k_{vR}}{k_{vc}} \tag{21}$$

Table 1
The conversion scales between the flow parameters in the LSM

Scale number	I	II	III	IV	V	VI	VII	VIII
Scale name	z_p	x_p	y_p	k_{hp}	k_{vp}	$\Re_p$	n_p	S_{sp}
Scale value	1	1	1	1	r^2 or e^{2R}	r^2 or e^{2R}	r^2 or e^{2R}	r^2 or e^{2R}

and, from Eq. (12),

$$\Re_p = \frac{Q_{zp} k_{vc} k_{hR}}{\phi_p^2 k_{vR} k_{hc}}. \tag{22}$$

The parameters involved are x_p, y_p, z_p, k_{hp}, k_{vp}, Q_{Rp}, Q_{zp}, $Q_{\theta p}$, t_p, n_p, ϕ_p and $\Re_p$ (12 parameters). And we have seven independent equations (Eqs. (17)–(22)). It means five parameters may be chosen arbitrarily. For example if we choose $\phi_p = 1$, $Q_{Rp} = 1$, $Q_{zp} = 1$, $Q_{\theta p} = 1$ and $t_p = 1$ then we will have $x_p = 1$, $y_p = 1$, $z_p = 1$, $k_{hp} = 1$, $k_{vp} = e^{2R}$, $\Re_p = e^{2R}$ and $n_p = e^{2R}$.

In these three cases to ensure that the quantities ϕ, Q_R, Q_z, Q_θ and t in the R-system and their equivalents (ϕ, Q_x, Q_z, Q_y, t) in the c-system are equivalent, we have to consider the following scales between the other parameters in the two systems:

(I) $z_p = 1$: the z scaling is identical for the two systems,
(II) $x_p = 1$ or $x_c/R = 1$ or $x_c/\ln(r) = 1$: the natural logarithm of r in the r-system is equivalent to x_c in the c-system.
(III) $y_p = 1$ or $y_c/\theta = 1$ or $y_c/r\theta = 1/r$: the $r\theta$-axis in the r-system must be multiplied by $1/r$ to be equivalent to the y_c-axis in the c-system.
(IV) $k_{hp} = 1$: the horizontal conductivity in the two (r and c) systems must be the same.
(V) $k_{vp} = e^{2R}$ or $k_{vc}/k_{vR} = r^2 = e^{2R}$: the vertical conductivity in the c-system must be a function of R in the R-system or a function of x_c in the c-system ($k_{vc} = k_{vR}e^{2R} = k_{vR}e^{2x_c}$)
(VI) $\Re_p = e^{2R}$ or $\Re_c/\Re_R = r^2 = e^{2R}$: the surface recharge for phreatic aquifers in the c-system must be a function of R in the R-system or a function of x_c in the c-system ($\Re_c = \Re_R e^{2R} = \Re_r e^{2x_c}$).
(VII) $n_p = e^{2R}$ or $n_c/n_R = r^2 = e^{2R}$: the specific yield or effective porosity in the c-system must be a function of R in the R-system or a function of x_c in the c-system ($n_c = n_R e^{2R} = n_R e^{2x_c}$).
(VIII) $S_{sp} = e^{2R}$ or $S_{sc}/S_{sR} = r^2 = e^{2R}$: the specific storage for a confined aquifer in the c-system must be a function of R in the R-system or a function of x_c in the c-system ($S_{sc} = S_{SR}e^{2R} = S_{sR}e^{2x_i}$).

Table 1 summarises the above scales.

For convenience, we refer to the above methodology and scalings as the log scaling method (LSM). In short, the LSM details the conversion of a simple two-dimensional (c-system) flow configuration in Cartesian coordinates to an equivalent axisymmetric cylindrical coordinate flow system (r-system). Using the LSM, we can simulate two-dimensional cylindrical flow systems very accurately within the (Cartesian) MODFLOW package.

3. Adoption of the LSM in MODFLOW

We consider the x_c, y_c and z_c axes in the Cartesian model (c-system) corresponding to the r, θ and z_r axes in cylindrical coordinates (r-system) (Fig. 1). To predict the axisymmetric flow to a well a slice of aquifer (Fig. 1(a)) is modelled. For the slice with $\Delta\theta = 1$, we consider one row of cells along the y_c-axis with DELC = 1 unit (scale III above) ($DELC_i$ is the cell width of row i in all columns [5], Table 2), NCOL columns along the x_c-axis with given DELR ($DELR_j$ is the cell width of column j in all rows [5], Table 2), which depends on the flow boundary condition as will be discussed later. We consider NLAY layers along the z_c-axis whose thicknesses are given and depend on the well screen boundary condition as will be discussed later. Note that, based on scale II, one point with $x_c = x_{c1}$ in the c-system corresponds to the point $r = e^{x_{c1}}$ in the r-system. The z-axis coordinates of the corresponding points in the two systems are the same (scale I). The well in the model is positioned by Well package in cells of the first row and column of the model and the flow of the well is divided in the well cells based on the cell layer thickness. The rate of flow to the well through the slice is $\Delta\theta/2\pi$ times the pumping rate.

The horizontal hydraulic conductivity in the c-system (k_{hc}) is set equal to the axisymmetric flow horizontal conductivity (k_{hR}) (scale IV).

The vertical conductivity in the c-system (k_{vc}) should be a function of both the x_c-axis and the vertical conductivity for axisymmetric flow (k_{vR}) (scale V). Based on this scaling, the average vertical hydraulic conductivity of a given cell whose boundary coordinates along the x_c-axis are x_{c1} and x_{c2} can be calculated as follows:

$$\overline{k_{vc}} = \frac{1}{x_{c2} - x_{c1}} \int_{x_{c1}}^{x_{c2}} k_{vR} e^{2x_c} \, dx_c = k_{vR} \frac{e^{2x_{c2}} - e^{2x_{c1}}}{2(x_{c2} - x_{c1})}. \tag{23}$$

For this cell in the c-system, the average value of $\Re_c$, n_c and S_{sc} are calculated in the same manner as Eq. (23).

Table 2
The MODFLOW parameters' definition and PCG solver parameter values commonly used in the simulations

Parameter name	Description	Value
$DELC_i$	The cell width of row i in all columns [5] (m)	See Table 3
$DELR_j$	The cell width of column j in all rows [5] (m)	See Table 3
PCG	Preconditioned conjugate-gradient package	See Table 3
MXITER	Maximum number of outer iterations	90
ITER1	Number of inner iterations	50
NPCOND	Matrix condition method	1
HCLOSE	The head change criterion of convergence	10^{-6}–0.005
RCLOSE	The residual criterion for convergence	10^{-6}–0.0001
RELAX	Relaxation parameter	1.0
NBPOL	The parameter for estimation of upper bound on the maximum eigenvalue	2.0
DAMP	Damping factor	0
DICREPANCY	The error in model inflow and out flow during a time step	See Table 3
NLAY	Number of layers	See Table 3
NROW	Number of rows	See Table 3
NCOL	Number of columns	See Table 3
PERLEN	The length of a stress period	See Table 3
NSTP	The number of time steps in a stress period	See Table 3
TSMULT	The multiplier for the length of successive time step	See Table 3

4. Simulation of axisymmetric flow using the LSM

The LSM was embedded in MODFLOW 2000 [5]. To study the accuracy of the LSM, the results simulated by MODFLOW for the three above-mentioned cases (Sections 2 and 2.1.1) are compared with their corresponding analytical solutions. The accuracy was expressed in terms of the relative error:

$$\text{Accuracy ratio in Percent} = \left(\frac{|h_L - h_A|}{J}\right) \times 100 \qquad (24)$$

where h_L is the numerical result, h_A is the analytical result and J is a reference value which may be the drawdown at the end of a pumping period or the drawdown in the well at a certain specific time.

For all the following cases PCG solver is used. The parameter setting of PCG solver is presented in Table 2. The simulations are done by use of Pentium-II, processor 500 MHz.

4.1. Steady confined flow

To determine the accuracy of the LSM in case of the flow with and without vertical component, we simulate the steady axisymmetric flow in a confined, homogeneous aquifer for two cases of fully and partially penetrating wells. The parameters for these simulations are presented in Table 3. The partially penetrating well screen is in the depth of 4.8–7.2 m. A constant head boundary is set for the both cases.

4.1.1. Fully penetrating well

To simulate this scenario using the LSM, a two-dimensional model with the discretization presented in Fig. 3(a) is used. In the model, the parameter DELR ranges from 0.171 to 0.264 m. As mentioned before cells in row 1 and column 1 of every layer present the well. For simulating the well radius of 0.4 m the outer boundary of the well cells must be at $x_c = \ln(0.4) = -0.9163$ m. The model parameters for each cell are computed based on the LSM. For example, if the cell is between $x_{c1} = 2.4849$ m and $x_{c2} = 2.7199$ m in the model (c-system) or $r_1 = 12.00$ m and $r_2 = 15.18$ m in the field (r-system), and $k_{vR} = 10^{-5}$ m/s, then the vertical hydraulic conductivity of this cell in the c-system (k_{vc}) will be $183.83 \times k_{vR} = 1.8383 \times 10^{-3}$ m/s (Eq. (23)). All other aquifer parameters in the c-system, (scales V to VIII) are calculated in the same manner. The results of this simulation for different radial distances, by MODFLOW (coupled with the LSM) and by the Thiem analytical formula [7] are presented in Fig. 4. There is a good agreement between the analytical solution and the LSM. For calculating the accuracy ratio here, we consider the reference parameter J equal to the hydraulic head at the constant head boundary (10 m). The average accuracy ratio between Thiem formula and the LSM from near the of well to 11 m from the well, is about 0.002%. The runtime for this case is less than 15 s (Pentium II, processor 500 MHz) with an overall total discrepancy of 0.0%. The results show that in the case of horizontal radial axisymmetric flow without vertical component the LSM generates almost exact results, Table 4 column 2).

4.1.2. Partially penetrating well

For the case of the partially penetrating well, only the well cells must be changed with other model parameters unchanged (Table 3). The well screen is in $z = 0.8$–3.2 m (depth of 4.8–7.2 m). The runtime for this case is less than 15 s with a total discrepancy of 0.0%. The results of the simulation for this condition in the form of a

Table 3
The aquifer and model parameters for different case studies

Aquifer and model parameters	Steady confined fully penetrated	Steady confined partially penetrated	Unsteady confined fully penetrated		Unsteady confined partially penetrated		Unsteady unconfined partially penetrated	
			LSM	Barrash and Dougherty [1]	Short time	Long time	Short time	Long time
b	8	8	8	8	8	8	8	8
k_h (m/s)	10^{-5}	10^{-5}	10^{-5}	10^{-5}	10^{-5}	10^{-5}	10^{-5}	10^{-5}
k_v (m/s)	10^{-5}	10^{-5}	10^{-5}	10^{-5}	10^{-5}	10^{-5}	10^{-5}	10^{-5}
S_s (m^{-1})			1.03155×10^{-3}	1.03155×10^{-3}	1.03155×10^{-3}	1.03155×10^{-3}	1.03155×10^{-3}	1.03155×10^{-3}
S_y	–	–	–	–	–	–	0.2	0.2
h_0 (m)	10	10	100	100	100	100	98	98
Q (m^3/s)	6.28×10^{-4}	6.28×10^{-4}	6.28×10^{-4}	6.28×10^{-4}	6.28×10^{-4}	6.28×10^{-4}	6.28×10^{-5}	6.28×10^{-5}
Screen interval (z) m	Full	0.8–3.2	0.8–3.2	0.8–3.2	0.8–3.2	0.8–3.2	0.8–3.2	0.8–3.2
r_w (m)	0.4	0.4	0.001	0.001	0.001	0.001	0.001	0.001
Ultimate r (m)	15	15	11,000	5300	11,000	39,000	11,000	39,000
NLAY	43	43	43	43	77	77	77	77
NROW	1	1	1	81	1	1	1	1
NCOL	15	15	60	41	43	43	43	43
DELC (m)	1	1	1	0.001	1	1	1	1
DELC (expansion factor)	1	1	1	1.44	1	1	1	1
DELR (m)	0.171–0.264	0.171–0.264	0.25	0.001	0.001	0.001	0.001	0.001
DELR (expansion factor)	–	–	1	1.44	1.4	1.4	1.4	1.4
Layer thickness (m)	0.2	0.2	0.2	0.2	0.001 on screen boundary	0.001 on screen boundary	0.001 on screen boundary	0.001 on screen boundary
Layer thickness (expansion factor)	1	1	1	1	1.4	1.4	1.4	1.4
Well location (row)	1	1	1	1	1	1	1	1
Well location (column)	1	1	1	1	1	1	1	1
Well location (layer)	All	26–38	All	All	24–60	24–60	24–60	24–60
Constant head location (row)	1	1	–	–	–	1	1	1
Constant head location (column)	15	15	–	–	–	43	43	43
Constant head location (layer)	All	All	–	–	–	All	All	All
PERLEN			19,943	19,943	19,943	6.602×10^{7}	19,943	6.602×10^{7}
NSTP			449	449	36	36	295	36
TSMULT			1.03663	1.03663	1.58489	1.58489	1.03663	1.58489

dimensionless drawdown factor $f(s)$ versus r/b [18] by the LSM and the results, which presented by Weeks [18] for different depths are given in Fig. 5. The results show good agreement at all depths. The small difference observed for L1 and L0.5 (8 and 4 m depths) is due to the concentration of the flow and high hydraulic gradient near the well screen margins.

4.2. Unsteady confined flow

For simulating unsteady confined axisymmetric flow, a confined, homogeneous aquifer was considered. Both a fully penetrating well and a partially penetrating well with a screen depth of 4.8–7.2 m were examined (Table 3). Because the analytical solutions take the well radius to be zero, the well radius in the LSM was set to 0.001 m.

4.2.1. Fully penetrating well

To consider the effect of aquifer specific storage we run the LSM model for confined and fully penetration condition. The model parameters used in the simulation of this case are presented in Table 3. DELR here is considered constant and equal to 0.25 m because the

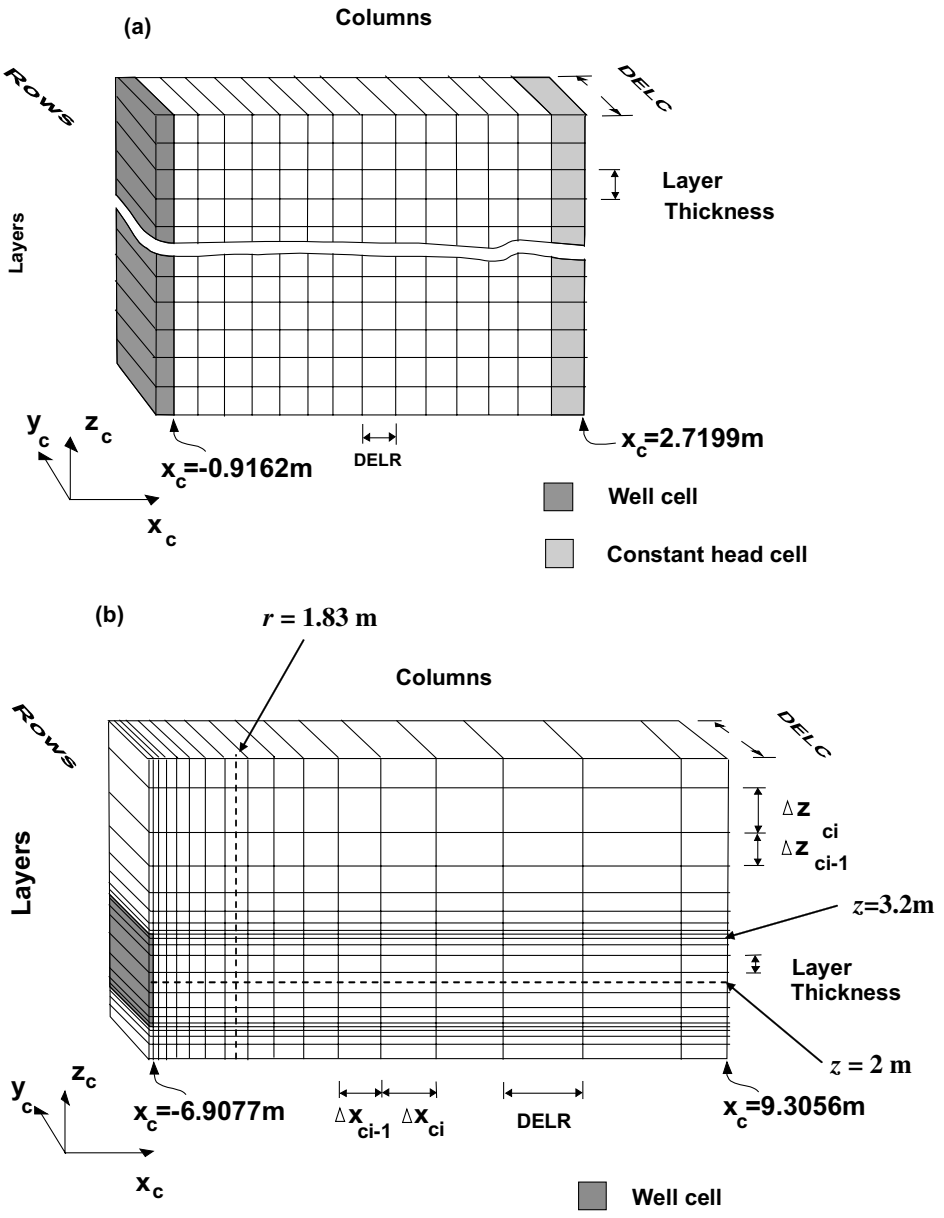

Fig. 3. Schematic diagrams showing the MODFLOW columns, rows and layers in the c-system, for simulating: (a) axisymmetric steady flow in a confined aquifer created by fully penetrating well and, (b) axisymmetric unsteady flow induced by a partially penetrating well.

well is fully penetrated and there is no concentration of the flow near the well. For simulating the well cells in the c-system it is only necessary that their outer boundaries be at $x_c = -6.9077$ m ($r = 0.001$ m). The aquifer length along the r or x_c-axis (along model rows) from centre of the well is assumed to be 11,000 m ($x_c = 9.3056$ m). So, the radius of influence of the well does not reach the aquifer boundaries. For improving the accuracy of the model simulation the time steps is considered very short (Table 3). The runtime for this case was less than 1 min with a −1.6% total discrepancy (Table 4). For calculating the accuracy ratio the parameter J is considered equal to the well drawdown at the end of pumping (12.5 m). The drawdown–distance curves for the pumping period of 19,943 s computed by MODFLOW (discretized by the LSM) and by the analytical model [16] are illustrated in Fig. 6. There is good agreement between analytical solution and the LSM. The average accuracy ratio from near the centre of the well to 41 m away from the well is about 0.077% (see Table 4).

For comparison, the above condition is also simulated by MODFLOW based on the Barrash and Dougherty [1] discretization scheme. The model parameters for this simulation are the same as for the above simulation and presented in Table 3. In this model DELC and DELR in the cells next to the well was set to 0.001 m; these values increasing by the expansion factor (α) of 1.44 moving away from the well. The

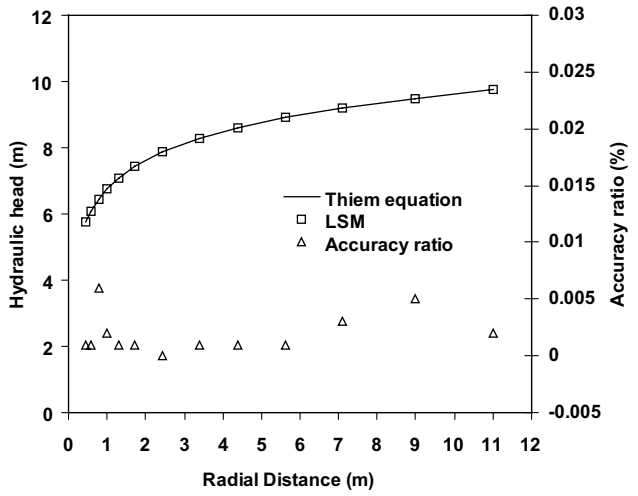

Fig. 4. Hydraulic head versus radial distance from the well axis for an 8 m thick confined aquifer discharged by a fully penetrating well. The heads are obtained by the LSM and by the Thiem formula [7].

expansion factor is a constant ratio that can be considered between the dimension of the successive cells in a certain direction in a model [1]. The runtime for this case is about 1 h with 2.8 % total discrepancy, Table 4.

The drawdown–distance curves for the pumping period of 19,943 s computed by the Barrash and Dougherty [1] discretization scheme and by the analytical model [16] and accuracy ratios are illustrated in Fig. 7. The J parameter here is equal to the well drawdown in the end of pumping. The average accuracy ratio between the two methods, from the well to 41 m away from the well, is about 3.7%. Relative to the LSM, the Barrash and Dougherty [1] results show lower accuracy and more computation time for simulating simple unsteady flow regime in a confined aquifer with a fully penetrating well, Table 4. It must be noted that simulation of the above case by RADMOD [13] is as accurate as by the LSM.

4.2.2. Partially penetrating well

To determine the effect of using expansion factor for considering concentration of flow near the well screen margins and also the effect of constant head we simulate confined and partially penetrating condition in this section. The simulation is conducted for two cases of with and without constant head boundary. The model parameters are shown in Table 3. To consider the effect of flow concentration near the well screen margins, the layer thickness was refined in the vicinity of the transition from the screened to the unscreened section of the well, and increased logarithmically away from it with $\Delta z_i/\Delta z_{i-1} = 1.4$ [14]. If DELR value in the cells next to the well is set considerably bigger than 0.001, a poor aspect ratio results with the long dimension be aligned along the direction of flow [1]. So, for cells next to the

Table 4
The simulation results for different cases and conditions

Aquifer and model parameters	Steady confined fully penetrated	Steady-confined-partially penetrated	Unsteady confined fully penetrated		Unsteady confined partially penetrated		Unsteady unconfinedpartially penetrated	
			LSM	Barrash and Dougherty [1]	Short time	Long time	Short time	Long time
Run time (s)	<15	<15	<60	3500	<60	<60	<60	<60
Total discrepancy (%)	0	0	−1.6	2.8	−4.17	−0.01	8.52	18.95
Location of observation one	$z = 1$ m	$z = 0$–8 m (0.8 m intervals)	$z = 1$ m	$z = 1$ m	$z = 2$ m	$z = 3.2$ ($r = 1.83$ m)	$z = 2$ m	$z = 3.2$ ($r = 1.83$ m)
Average accuracy ratio (%) for observation point one (range of averaging)	0.002 ($r = 0.4$–11 m)	–	0.077 ($r = 0.001$–41 m)	3.7 ($r = 0.001$–47 m)	0.904 ($r = 0.001$–100 m)	1.249 ($t = 2.4$–6.602×10^7 s)	1.415 ($r = 0.001$–100 m)	0.709 ($t = 2.4$–6.602×10^7 s)
Location of observation point two	–	–	–	–	$z = 3.2$ m	–	$z = 3.2$ m	–
Average accuracy ratio for observation point two (range of averaging)	–	–	–	–	0.467 ($r = 0.001$–100 m)	–	0.134 ($r = 0.001$–100 m)	–

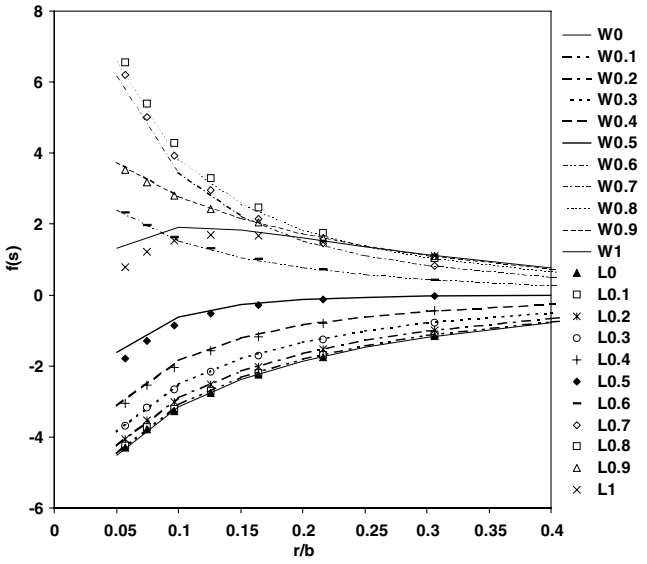

Fig. 5. The dimensionless drawdown factor $f(s)$ versus r/b [18], for a confined aquifer discharged by a partially penetrating well. The $f(s)$ results are obtained from the LSM and from the data presented by Weeks [18]. (W0.1 means: Weeks solution at $d/b = 0.1$; L0.3 means: LSM at $d/b = 0.3$.

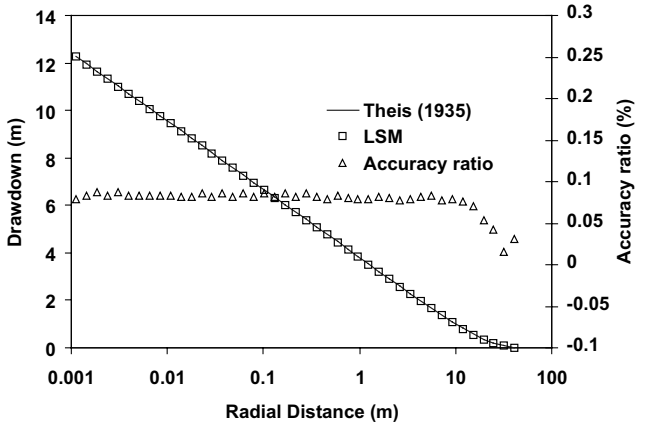

Fig. 6. Drawdown–distance plot for a confined aquifer discharged by a fully penetrating well. Drawdown is obtained by the LSM and by the Theis [16] method.

well we set DELR = 0.001 m while DELC increases logarithmically away from the well with $\Delta x_{ci}/\Delta x_{ci-1} = 1.4$ (Fig. 3(b)). The model was run for a short time period of $t = 19{,}943$ s and with no constant head boundary at the far distance from the well. The runtime for this case is less than 60 s with a −4.17% total discrepancy. The drawdown–distance curves for the two elevations (z) of 2 and 3.2 m (Fig. 3(b)) for a pumping period of 19,943 s by the LSM and by the analytical solution [4] are illustrated in Fig. 8. There is a good agreement between analytical solution and the LSM. The average accuracy ratios for the elevation of 2 and 3.2 m to the

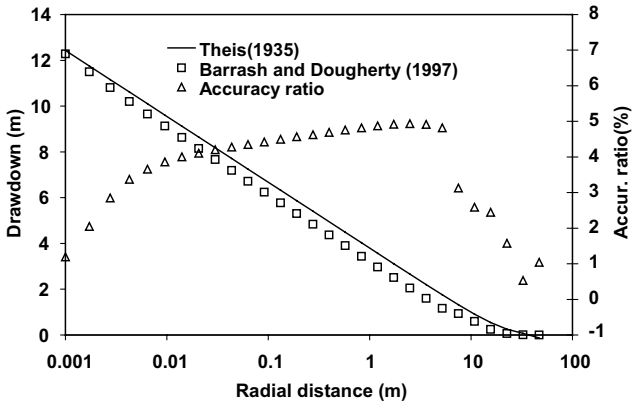

Fig. 7. Drawdown–distance plot for a confined aquifer discharged by a fully penetrating well. Drawdowns are obtained by the Barrash and Dougherty [1] discretization scheme and by the Theis [16] method.

radius of 100 m from the well are about 0.904% and 0.467%, respectively Table 4. The J parameter here is equal to the well drawdown (27 m). It can be seen in Fig. 8 that close to the well the accuracy ratio increases. As mentioned in Section 4.1 this increase in accuracy ratio is due to the concentration of the flow near the well screen. Here because of considering expansion factor in the cells discretization, the accuracy ratios are less than 1.5% even very close to the well. Also, For the points at the middle of the well screen ($z = 2$ m) more accuracy ratio can be seen (Fig. 8) relative to the points at the margin of the well screen ($z = 3.2$ m). This is because of the poor aspect ratio of the model cells located in the middle of the screen. Because the layer thickness near the margin of the well screen set to 0.001 m and increased with expansion factor of 1.4 to the middle of screen.

To study the effect of length of pumping period and number of time steps and also the effect of constant head in reducing the total discrepancy of the model, a par-

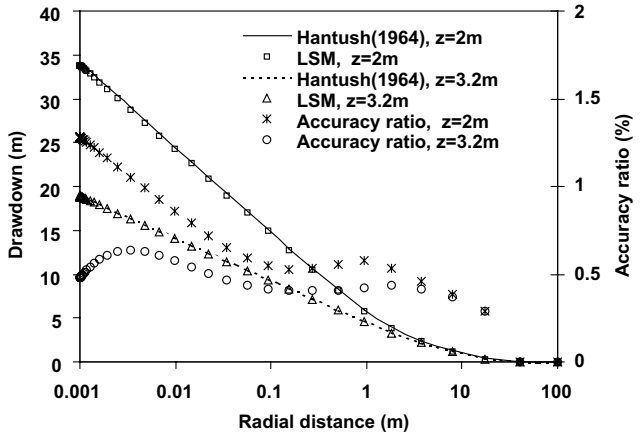

Fig. 8. Drawdown–distance plot for a confined aquifer discharged by a partially penetrating well. Drawdowns are obtained for $z = 2$ and 3.2 m, by the LSM and by the Hantush [4] method.

tially penetrating well in a confined aquifers with the same parameter set (Table 3) but with constant head and a pumping period of $t = 6.60192 \times 10^7$ s was run. The drawdown–time curves for $z = 3.2$ m and $r = 1.83$ m during the time interval of 6.60192–6.60192×10^7 s for both the LSM and the analytical method [4] are illustrated in Fig. 9. The total discrepancy for this case is −0.01%. It can be seen that by applying constant head the total discrepancy deceased considerably relative to the short time case. The accuracy ratios for the results of the two methods are also shown in Fig. 9. The J parameter here is equal to the drawdown at observation point at the end of pumping (10 m). There is a good agreement between the analytical solution and the LSM. The average accuracy ratio for the results obtained after 2.4 s from beginning of pumping is about 1.249% (see Table 4).

4.3. Unsteady unconfined flow to a partially penetrating well

To study the effect of specific yield and the time discretization on the accuracy of the LSM, an unconfined homogeneous aquifer discharged by a partially penetrating well is considered (Table 3). The simulation here is done for two cases of short and long time. In short time case the model has more time steps with shorter time intervals and in long time case the model has less time steps with longer time intervals (Table 3). Also the constant head for both cases are considered. All other parameters are the same for both cases. Here the same expansion factor as in Section 4.2.2 is considered for discretization of layers and columns.

For short time case the simulation is done for $t = 19{,}943$ s. To minimize the discrepancy we increased the number of time steps to 295, decreased the time multiplier to 1.036632928 and also decreased values of HCLOSE and RCLOSE parameters in PCG solver to their possible minimum value (that model can handle) of 0.005 and 0.0001 respectively. But we could not decrease the total discrepancy less than 8.52%. By following the variation of discrepancy during the time steps in this case we found that the maximum discrepancy belongs to the transition times when the specific yield starts supplying the well discharge. At these times there is a sudden change in the slope of drawdown–time type curve of unconfined aquifers [9]. On the other hand the MODFLOW time discretization is designed so that the time steps will be longer in late times (TSMULT), as the model expects a lower amount of change in drawdown. Therefore, in the case of radial flow in unconfined aquifers, the sudden increase in the slope of drawdown–time curve during transient times causes a considerable error and increase in the total discrepancy.

For the short time case the drawdown–distance curves for $z = 2$ and 3.2 m, during the pumping period of 19,943 s computed by the LSM and by the analytical solution [9] together with their accuracy ratio, are illustrated in Fig. 10. For calculating accuracy ratio in this case, J is considered equal to the well drawdown (2.5 m). In spite of the large discrepancy in the model simulation, there is a very good agreement between analytical solution and the LSM. The average accuracy ratio between the two methods for elevations (z) of 2 and 3.2 m to a distance of 100 m from the well are 1.415% and 0.134%, respectively Table 4. Fig. 10 also shows increase in accuracy ratio close to the well as in Fig. 8. Fig. 10 shows higher accuracy ratio for the points with $z = 2$ m relative to the points with $z = 3.2$ m w because of poor aspect ratio in cells at $z = 2$ as in Section 4.2.2.

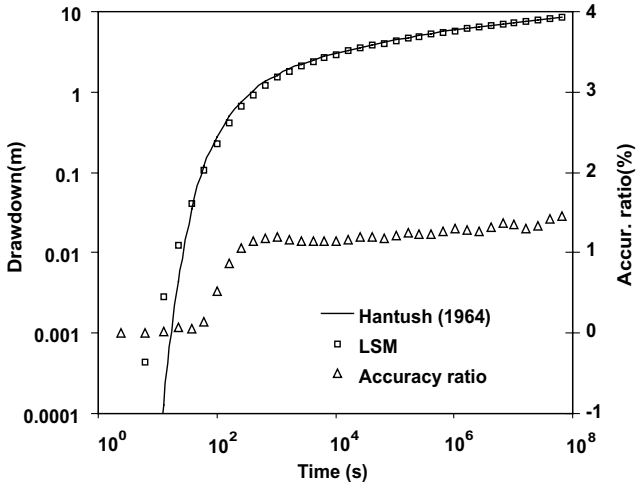

Fig. 9. Drawdown–time plot for a confined aquifer discharged by a partially penetrating well. Drawdowns are obtained by the LSM and by the Hantush [4] method for $z = 3.2$ m and $r = 1.83$ m.

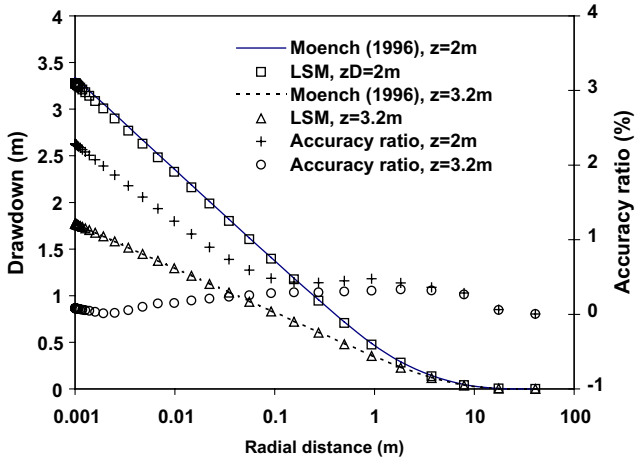

Fig. 10. Drawdown–distance plot for an unconfined aquifer discharged by a partially penetrating well. Drawdowns are obtained for $z = 2$ and 3.2 m, by the LSM and by the Moench [9] method.

For the long time case the above model was run for 36 time steps up to 6.60192×10^7 s with the time multiplier 1.584893192. The simulation results in 18.95% total discrepancy. This high amount of discrepancy shows the effect of time discretization in the model discrepancy for unconfined aquifer case and the contribution of S_y in supplying water to the well. Time-drawdown curves for $z = 3.2$ and $r = 1.83$ for a pumping period of 6.60192–6.60192×10^7 s (with 36 steps) computed by the LSM and the analytical method [9] are plotted in Fig. 11. Also the accuracy ratio of the two methods with respect to time is shown (Fig. 11). The J parameter here is equal to the drawdown at end of pumping time (1 m). For this case also a good agreement between analytical solution and the LSM can be seen. The average accuracy ratio after 2.4 s from the beginning of pumping is about 0.709%, Table 4. As discussed for the short time case the maximum error is seen in the transition time in Fig. 11.

To reduce the total discrepancy in long time case we ran the model for the period after the transition time. For this, we changed the NSTP parameter in the model from 36 to 13 time steps. By this change, the beginning time of the simulation changes to 9.7×10^4 s automatically. Then the total discrepancy reduced to −0.22%. This result reconfirms that the sudden change in the curve slope during $t = 10^4$–10^5 s in Fig. 11 creates large total discrepancy in long time case.

It must be noted that in simulation of the above cases it is assumed that the model cells near the water table can be dried due to increase of drawdown. Simulation of the above case by RADMOD is not possible.

5. Summary and conclusions

Groundwater numerical models with conventional rectilinear grid geometry such as MODFLOW generally have not been used to simulate groundwater flow in the vicinity of wells. To simulate axisymmetric flow to pumping wells by numerical models a new method called the LSM was formulated and coupled with MODFLOW 2000. The formulation is based on the similarity of the equations and boundary conditions describing the flow behavior in cylindrical and Cartesian coordinates, resulting in a set of relationships and scales that were employed for the conversion of one system to the other. Similar scaling conversions have been adopted for converting anisotropic aquifer to isotropic aquifer system in simulating groundwater flow beneath dams [2].

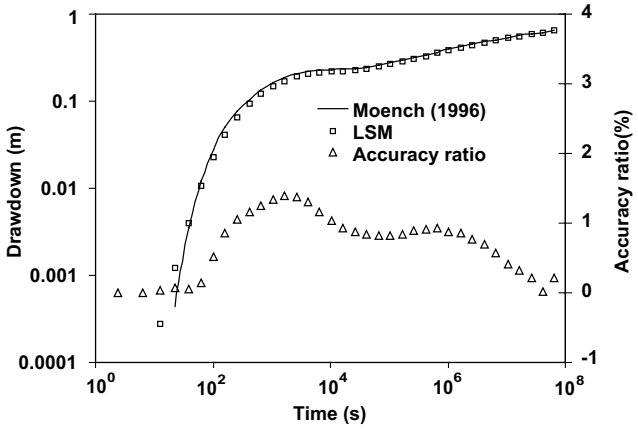

Fig. 11. Drawdown–time plot for an unconfined aquifer discharged by a partially penetrating well. Drawdowns are obtained by the LSM and by the Moench [9] method for $z = 3.2$ m and $r = 1.83$ m.

The method was applied to steady, unsteady, confined, unconfined, fully and partially penetrating wells with and without constant head boundary, with and without applying expansion factor in cell discretization and with different time discretization schemes. The results were compared with the corresponding analytical solutions and showed a high degree of accuracy. The accuracy ratio in all cases is less than 1.5%. For the case of steady and unsteady flow with fully penetrated well the LSM shows almost the exact results and it's accuracy is not depend on the cells' discretization schemes. In the case of partially penetrating well applying the expansion factor for discretization of the layers and the columns and also consideration of constant head boundary at far distance reduce effectively the total discrepancy of the model and the accuracy of the results. The increase of the accuracy ratio with decreasing distance to the well in partially penetrating cases is due to vertical component and concentration of flow near the well screen. The concentration of flow near the screen margins also can be seen in the two-dimensional flow and is not because of the radial flow, therefore it must not be expected that it can be eliminate completely by the LSM method. But by considering expansion factor in cell's discretization the effect of flow concentration error reduces and an accuracy ratio less than 1.5% is achieved.

In the case of unconfined partially penetrating well the accuracy ratio is less than 1.5% but the total discrepancy of the model is high. The high amount of the error in simulating the radial flow by MODFLOW is because the time step interval of the model increases during the time by a time multiplying factor (TSMULT) and the model expects less drawdown change during a certain time interval in late times. Therefore the sudden change in drawdown–time curve slope in transition times in unconfined radial flow due to contribution of S_y in supplying water to the well causes considerable error in the model results and hence increase in total discrepancy. In simulating unconfined radial flow by the LSM, shortening the time steps causes reduction of total discrepancy to less than 8.52% and ignoring the transition time reduces it to 0.22%.

The method is more general, efficient and accurate for simulating axisymmetric flow than the scheme presented by Barrash and Dougherty [1], and employed in RADMOD [13]. The Barrash and Dougherty [1] scheme is empirical and based on a trial-and-error procedure, with a suggested constant expansion factor of 1.2–1.5 for the mesh spacing. In contrast, the proposed method is theoretically based on geometry and physical properties of aquifer flow. In the LSM, the mesh spacing is based on the flow geometry and the flow parameters for each cell are established using given scale factors. In other words, the mesh spacing is not dictated by the user but by the flow condition. In addition, the method is adaptable to all MODFLOW packages, and in simulating a phreatic aquifer, in contrast to RADMOD it has the capability to dry cells located above the water table boundary. The LSM method can be used for simulating flow in axisymmetrically nonhomogeneous aquifers like horizontal layered aquifers. The well boundaries like well storage and skin effect can be accurately simulated by the LSM. Also this method can be used for aquifers bounded by axisymmetric boundaries and well boundaries for which analytical solution does not exit.

The method cannot handle nonaxisymetric flow caused by aquifer nonhomogenities, but in many cases nonhomogenity and boundaries around the well can be assumed axisymmetric.

Acknowledgements

This paper was completed when the first author was on a sabbatical leave at the University of Edinburgh, UK. Financial support provided by Shiraz University, Iran is acknowledged. Useful comments and suggestions given by four anonymous reviewers are appreciated.

References

[1] Barrash W, Dougherty ME. Modeling axially symmetric and nonsymmetric flow to a well with MODFLOW, and application to Goddard2 well test, Boise, Idaho. Ground Water 1997;35(4): 602–11.

[2] Bear J, Dagan G. The relationship between solutions of flow problems in isotropic and anisotropic soils. J Hydrol 1965;3:88–96.

[3] Bennet GD, Reilly TE, Hill MC. Technical training note in ground-water hydrology: radial flow to a well. US Geological Survey Water-Resources Investigations Report: 89-4134, 1990, p. 83.

[4] Hantush MS. Hydraulics of wells. In: Chow VT, editor. Advances in hydroscience, vol. 1. New York: Academic Press; 1964. p. 281–432.

[5] Harbaugh AW, Banta ER, Hill MC, McDonald MG. MODFLOW-2000. The US Geological Survey modular ground-water model-user guide to modularization concepts and the ground-water flow process. US Geol. Survey: Open File Report 00-92, 2000.

[6] Johnson GS, Cosgrove DM, Frederick DB. A numerical model and spreadsheet interface for pumping test analysis. Ground Water 2001;39(4):582–92.

[7] Lee TC. Applied mathematics in hydrogeology. Boca Raton, LA, United States: Lewis Publishers; 1999.

[8] Lindner JB, Reilly TE. Analysis of three tests of the unconfined aquifer in southern Nassau County. Long Island, New York: US Geological Survey Water-Resources Investigations Report 82-4021, 1983, 51 pp.

[9] Moench AF. Flow to a well in a Water-table aquifer: an improved Laplace transform solution. Ground Water 1996;34(4):593–6.

[10] Mundorff MJ, Bennett GD, Ahmad M. Electric analog studies of flow to wells in the Punjab aquifer of West Pakistan. US Geological Survey Water-Supply Paper 1608-N, 1972, 28 pp.

[11] Pandit A, Aoun JM. Numerical modeling of axisymmetric flow. Ground Water 1994;32(3):458–64.

[12] Reilly TE. A Galerkin finite element flow model to predict the transient response of a radially symmetric aquifer. US Geological Survey Water-Supply Paper 2198, 1984, 33 pp.

[13] Reilly TE, Harbaugh AW. Simulation of cylindrical flow to a well using the US Geological Survey Modular Finite-Difference Ground-Water Flow Model. Ground Water 1993;31(3):489–94.

[14] Ruud NC, Kabala ZJ. Response of a partially penetrating well in a heterogeneous aquifer: integrated well-face flux vs. uniform well-face flux boundary conditions. J Hydrol 1997;194:76–94.

[15] Stallman RW. Electric analog of three-dimensional flow to wells and its application to unconfined aquifers. US Geological Survey Water-Supply Paper 1536-H, 1963, 37 pp.

[16] Theis CV. The relation between the lowering of the piezometric surface and the rate and duration of discharge of a well using groundwater storage. Trans Amer Geophys Union 1935;16:519–24.

[17] Todd DK. Ground water hydrology. New York: John Wiley & Sons; 1959.

[18] Weeks EP. Determining the ratio of horizontal to vertical permeability by aquifer-test analysis. Water Resour Res 1969; 5(1):196–214.